Evolutionary transition from degenerate to nonredundant cytokine signaling networks supporting intrathymic T cell development

Divine-Fondzenyuy Lawir[a], Isabell Hess[a], Katarzyna Sikora[a], Norimasa Iwanami[a,1], Iliana Siamishi[a], Michael Schorpp[a], and Thomas Boehm[a,2]

[a]Department of Developmental Immunology, Max Planck Institute of Immunobiology and Epigenetics, D-79108 Freiburg, Germany

Edited by Alain Fischer, Institut Imagine, Paris, France, and approved November 11, 2019 (received for review September 2, 2019)

In mammals, T cell development critically depends on the IL-7 cytokine signaling pathway. Here we describe the identification of the zebrafish ortholog of mammalian IL-7 based on chromosomal localization, deduced protein sequence, and expression patterns. To examine the biological role of *il7* in teleosts, we generated an *il7* allele lacking most of its coding exons using CRISPR/Cas9-based mutagenesis. *il7*-deficient animals are viable and exhibit no obvious signs of immune disorder. With respect to intrathymic T cell development, *il7* deficiency is associated with only a mild reduction of thymocyte numbers, contrasting with a more pronounced impairment of T cell development in *il7r*-deficient fish. Genetic interaction studies between *il7* and *il7r* mutants, and *il7* and *crlf2*(*tslpr*) mutants suggest the contribution of additional, as-yet unidentified cytokines to intrathymic T cell development. Such activities were also ascertained for other cytokines, such as il2 and il15, collectively indicating that in contrast to the situation in mammals, T cell development in the thymus of teleosts is driven by a degenerate multicomponent network of γ_c cytokines; this explains why deficiencies of single components have little detrimental effect. In contrast, the dependence on a single cytokine in the mammalian thymus has catastrophic consequences in cases of congenital deficiencies in genes affecting the IL-7 signaling pathway. We speculate that the transition from a degenerate to a nonredundant cytokine network supporting intrathymic T cell development emerged as a consequence of repurposing evolutionarily ancient constitutive cytokine pathways for regulatory functions in the mammalian peripheral immune system.

thymus | cytokine signaling | evolution | zebrafish | network structure

In mice, intrathymic T cell development is critically dependent on the presence of the IL-7 cytokine (1); in *Il7*-deficient mice, thymic cellularity is reduced by more than 20-fold (2). IL-7 belongs to the so-called γc cytokines, and its receptor is a heterodimer composed of the IL-7 receptor α chain and the common γ chain (γ_c), also known as IL-2RG (3). In mice mutant for the IL-7 receptor α chain, total thymic cellularity varied between 0.01% and 10% of wild-type levels (4); likewise, in mice mutant for γ_c, thymic cellularity is reduced by more than 30-fold (5). These findings identify IL-7 as the key cytokine stimulating the proliferation of thymocytes and suggest that it signals through the heterodimeric IL-7R/IL-2RG receptor (3). Likewise, in humans, lack of IL-7 is associated with severe T cell lymphopenia (6), and the same phenotype is observed in IL-7R (7) and IL-2RG (8) deficiencies. Collectively, these observations indicate that IL-7 is part of a nonredundant cytokine signaling network required for the development and maintenance of T cells in mammals. Of note, in contrast to the situation with T cell development, the requirement for IL-7 signaling in B cell development varies and is species-dependent; for instance, whereas B cells fail to develop properly in mice lacking IL-7, B cell development is not affected in humans with IL-7 deficiency (2, 7). These observations suggest a certain degree of functional flexibility in lymphoid-specific cytokine networks.

The results of large-scale forward genetic screens in zebrafish (9, 10) suggest that IL-7 signaling is also important for T cell development in lower vertebrates. In this screen, we identified lines deficient for *il7r*, *jak1*, and *jak3* genes, all exhibiting reductions in thymocyte numbers, resulting in peripheral lymphopenia; moreover, genetic interaction analyses suggested that *il7r*, *jak1*, and *jak3* act in the same pathway (10). Others have shown that a deficiency of 1 of 2 zebrafish *il2rg* genes causes a severe block in T cell development (11). Collectively, these results are compatible with the notion of a strong evolutionary conservation of the IL-7R–IL2-RG–JAK3 signaling pathway in vertebrate T cell development.

When viewed from the perspective of network design, the IL-7–(IL-7R–IL-2RG)–JAK3 signaling axis underlying mammalian T cell development appears to be remarkably brittle, despite the fact that T cells are of central importance for the immune defense of vertebrates. The apparent nonredundancy of the IL-7–(IL-7R–IL-2RG)–JAK3 signaling axis in T cells is mirrored in the nonredundant function of the FOXN1 transcription factor, which is essential for differentiation of the mammalian thymic microenvironment (12, 13), including provision of the IL-7 cytokine (14). Lack of *Foxn1* also causes catastrophic immunodeficiency

Significance

In mammals, intrathymic T cell development strictly depends on the activity of the IL-7 cytokine signaling pathway, leading to catastrophic immunodeficiency when even 1 of the components in the pathway fails. Here we report the unexpected observation that the development of T cells in the thymus of the teleost *Danio rerio* (zebrafish) is instead supported by the collective actions of several cytokine signaling pathways, with IL-7 signaling playing only a minor role. This finding suggests that during the course of evolution, a degenerate network was converted into a state of precarious brittleness, possibly because some of the evolutionarily ancient constitutive cytokine pathways had to be repurposed to meet increased demands for sophisticated regulation during the mammalian immune response.

Author contributions: D.-F.L., I.H., M.S., and T.B. designed research; D.-F.L., I.H., N.I., I.S., and M.S. performed research; D.-F.L., I.H., K.S., N.I., I.S., M.S., and T.B. analyzed data; and D.-F.L. and T.B. wrote the paper.

The authors declare no competing interest.

This article is a PNAS Direct Submission.

Data deposition: RNA-seq data have been deposited in the Gene Expression Omnibus (GEO) database, https://www.ncbi.nlm.nih.gov/geo (accession no. GSE136250).

[1]Present address: Department of Regenerative Medicine, National Center for Geriatrics and Gerontology, Obu City 474-8511, Japan.

[2]To whom correspondence may be addressed. Email: boehm@ie-freiburg.mpg.de.

This article contains supporting information online at https://www.pnas.org/lookup/suppl/doi:10.1073/pnas.1915223116/-/DCSupplemental.

First published December 10, 2019.

resulting from agenesis of the stromal microenvironment essential for mammalian T cell development.

While these findings suggest that the genetic network of T cell development is essentially nonredundant in mammals, there are indications that this might not be true for T cell development in teleosts. For instance, in contrast to the situation in mammals, the *foxn1* transcription factor gene of teleosts is not essential for thymopoiesis; in fact, coexpression in thymic epithelial cells of its paralog, *foxn4*, directs a substantial amount of lymphoid development in *foxn1*-deficient fish (15). In addition, *il7*-deficient fish were conspicuously absent in the collection of mutant lines of our large-scale forward genetic screen (9). Although there are trivial reasons for this outcome, we entertained the possibility that *il7* deficiency might have only a mild or no phenotype and thus would not have been detected under the stringent phenotypic selection criteria of the genetic screen. Therefore, we set out to determine the phenotype of *il7*-deficient zebrafish to examine the possibility that the cytokine signaling network in the thymus of teleosts might exhibit features of robustness not apparent from previous studies.

Here we report that, in contrast to mammals, T cell development in zebrafish is regulated by the collective activity of several γc cytokines, and discuss the adaptive value of this degenerate network design.

Results

Identification of the Zebrafish *il7* Gene. We identified ENSDARG00000092045 on chromosome 24 as a likely candidate for the zebrafish *il7* gene, initially based on the evolutionarily conserved synteny between *IL7* and *ZC2HC1A* genes that appears to hold for all jawed vertebrates, from sharks (16) to humans (http://useast.ensembl.org/index.html) (*SI Appendix*, Fig. S1*A*). Indeed, conceptual translation of the associated transcripts (*SI Appendix*, Fig. S1 *B* and *C*) indicates a close similarity to previously identified IL-7 homologs in lower vertebrates and to mammalian IL-7 (*SI Appendix*, Fig. S1 *D* and *E*). No other IL-7–related sequence was found in publicly available sequence collections and our own datasets, suggesting that only a single *il7*-like gene is present in zebrafish.

We next examined the expression of the putative zebrafish *il7* gene in the thymus and the kidney, the 2 key lymphopoietic sites in adult zebrafish. As expected, strong expression was found in the thymus (Fig. 1*A*) and in scattered regions of the kidney (Fig. 1*B*). Collectively, these results strongly suggest that ENSDARG00000092045 represents the *il7* homolog of zebrafish.

Phenotype of *il7*-Deficient Zebrafish. In an initial effort to explore the functional role of *il7* during T cell development, we examined the phenotype of *il7* morphants at 5 d postfertilization (dpf). The RNA in situ signal for *rag1*-expressing cells in the thymus was normalized to that of growth hormone gene (*gh*)-expressing cells

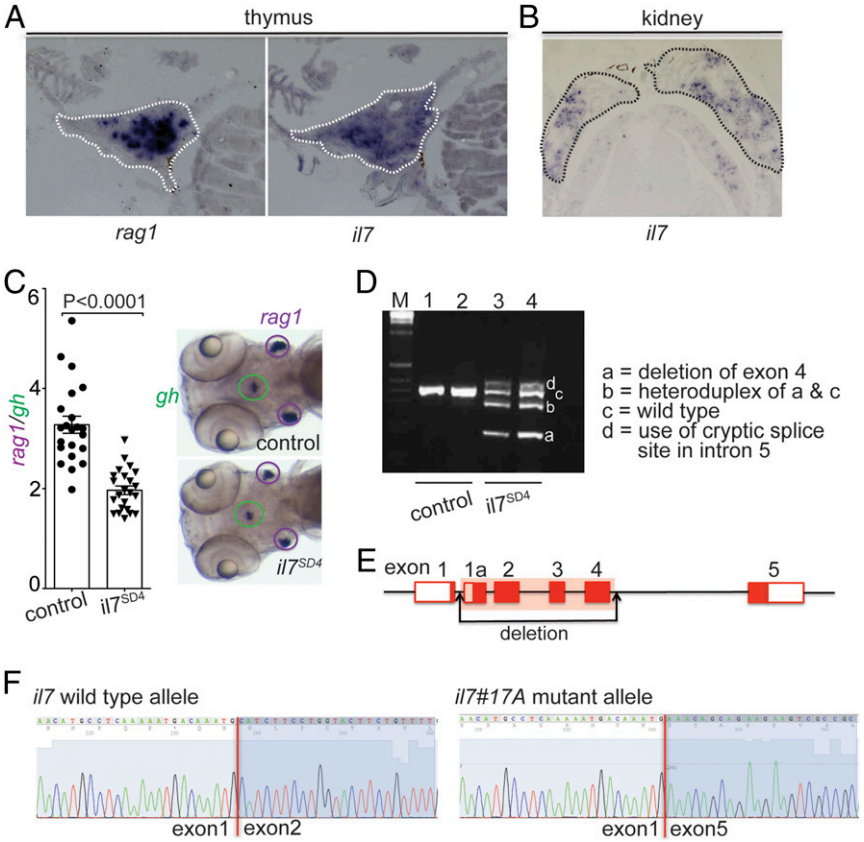

Fig. 1. Characterization of the zebrafish *il7* gene (ENSEMBL ID: ENSDARG00000092045). (*A*) RNA in situ hybridization on tissue sections of adult zebrafish thymus with probes specific for *rag1* and *il7*. (*B*) RNA in situ hybridization on tissue sections of adult zebrafish kidney with a probe specific for *il7*. (*C*) Reduced thymopoietic activity in *il7* morphants as determined by the thymopoietic index (*Left*), derived from quantitative analysis of whole-mount RNA in situ hybridization experiments (*Right*). Each data point represents 1 fish; data are mean ± SEM. (*D*) RT-PCR analysis of *il7* cDNA structures resulting from interference with splicing of the pre-mRNA transcripts by an antisense oligonucleotide targeting the splice donor site of exon 4 (SD4). The deletion in variant a does not cause a frame shift, since all exons of the *il7* gene are in phase 0; the use of cryptic splice site in the intron between exons 4 and 5 causes a frame shift mutation. (*E*) Schematic of the *il7* gene structure, indicating the deletion introduced by CRISPR/Cas9 mutagenesis. (*F*) Sequence analysis of cDNAs demonstrating the loss of sequences derived from exons 2 to 4 in transcripts emanating from the *il7#17A* mutant allele.

in the hypophysis, and the extent of thympopoietic activity was expressed as the *rag1*/*gh* ratio. The results, shown in Fig. 1*C*, indicate a surprisingly mild reduction of *rag1*-expressing cells of ∼30%. However, despite the presence of an antisense morpholino targeting the splice donor site of exon 4, a small fraction of pre-mRNAs was properly spliced (Fig. 1*D*); thus, we considered the possibility that the phenotype of *il7* morphants might be the result of a hypomorphic rather than an amorphic constellation. To circumvent this problem, we generated *il7*-deficient zebrafish using the CRISPR/Cas9 method of mutagenesis. The *il7#17A* allele exhibits a large deletion in the ENSDARG00000092045 locus, removing exons 2 to 4 (Fig. 1*E* and *SI Appendix*, Figs. S1 *B* and *C* and S2*A*), as demonstrated by cDNA cloning (Fig. 1*F*) and RNA sequencing (*SI Appendix*, Fig. S2 *B* and *C*).

The *il7* mutants were viable and appeared grossly normal (Fig. 2*A*); this phenotype is in line with the only minor changes seen in the transcriptomes of mutant fish when analyzed at 5 dpf (for whole larvae) and 3 mo (for whole kidney marrow) (Fig. 2*D* and *SI Appendix*, Table S1). At 63 h postfertilization (hpf)—that is, approximately 10 h after colonization of the thymic rudiment has begun (17)—the lack of *il7* was associated with small reductions of the numbers of *ikaros*-expressing T cell precursors in the thymic rudiment (Fig. 2*B*). This phenotype persisted, such that at 5 dpf, the number of *rag1*-expressing cells in the thymus was still reduced in the mutants (Fig. 2*C*). This effect is very similar in magnitude to the phenotype of *il7* morphants (Fig. 1*C*).

When examined at successively later stages of development, hematopoietic lineages in mutant fish appeared to be essentially normal, with the exception of slightly reduced numbers of *ikaros*-expressing lymphoid precursors in the thymus (Fig. 2 *D* and *E*). However, in contrast to the situation in mice, where the γδ T cell lineage is absolutely dependent on IL-7 (18), both αβ and γδ T cells appeared to be present in the mutant thymus, as determined by RNA in situ hybridization on tissue sections of adult fish (Fig. 2 *F*–*J*). Notably, B cell development in the kidney marrow also appeared to be intact, as demonstrated by the normal numbers of *ikaros*-expressing cells (Fig. 3 *A* and *B*); likewise, no differences were found between wild-type fish and *il7* mutants in the numbers of cells expressing *rag1* and *igm* (as markers of the B cell lineage) and *tcrb* and *tcrd* (as markers of the 2 principal lineages of T cells) in the kidney, as determined by RNA in situ hybridization of tissue sections (Fig. 3 *C*–*F*). Finally, the conclusion of unaltered lymphoid lineage specification in the absence of *il7* is supported by the presence of expressed complete assemblies of *tcrd*, *tcrb*, *igz*, and *igm* antigen receptor genes (Fig. 3*G*).

Genetic Network Analysis of *il7*. To further substantiate the functional assignment of the *il7* gene in the context of cytokine signaling, a genetic interaction analysis was carried out. Genetic interaction is defined as an unexpected phenotype created by combining the effects of 2 genetic variants, where an experimentally observed double-mutant phenotype is less severe (positive or alleviating interaction) or more severe (negative or synthetic interaction) than an expected value predicted from both single mutant phenotypes (19). A positive interaction often indicates that 2 genes operate in the same pathway, as we have shown previously for *il7r* and *jak3* using this method (10).

Again, the thymopoietic activities in *il7r;il7* and *jak3;il7* double mutants were much greater than expected from the independent activities of the 2 mutations on the outcome of T cell development (Fig. 4 *A*–*D*). The observed positive genetic interactions thus indicate that *il7*, *il7r*, and *jak3* genes jointly act in the same pathway, strongly supporting the notion that the ENSDARG00000092045 gene encodes the zebrafish *il7* homolog. However, the genetic interaction analysis described above provided no explanation for the discrepant phenotypes of *il7* mutants on the one hand and *il7r* mutants on the other hand. A possible explanation for the more severe phenotype of the *il7r* mutant could be that the il7r α chain —in zebrafish as in the mouse—is also part of a second receptor, in complex with a CRLF2-like receptor chain, known as the TSLP receptor in mammals (20).

Since a functional equivalent of mammalian TSLP has not yet been found in zebrafish, we examined the effect of a deficiency of the zebrafish *crlf2*-like gene (Fig. 4*E*) on T cell development in the thymus. As shown in Fig. 4 *F* and *G*, *crlf2*-deficiency strongly impairs T cell development in zebrafish larvae, although the magnitude of reduction in T cell development is less than that observed for *il7r* mutants (10); in contrast, TSLP-signaling contributes only minimally to intrathymic T cell development in mice (21). Since *il7* and *crlf2* genes do not interact (Fig. 4 *F* and *G*), they appear to function independently to regulate T cell development in the zebrafish thymus. Taken together, these observations suggest the presence of an as-yet unidentified cytokine (possibly a functional equivalent of TSLP in zebrafish) that signals through the il7r/crlf2 complex and substantially contributes to intrathymic T cell development. Conceptually, this result suggests an unexpected level of redundancy of cytokine function in zebrafish thymopoiesis instead of the dominant role of IL-7 in mammalian T cell development.

Interestingly, *tcrd* rearrangements are absent in *il7r* mutants but not in *il7* mutants (Fig. 3*D*), suggesting that il7 and the putative crlf2 ligand both contribute to the formation of the γδ T cell lineage, and that their simultaneous absence (or the lack of Il7r serving as their common receptor component) is needed to abolish the development of γδ T cells. This contrasts with the situation in mice, where the lack of only IL-7 already results in failure of γδ T cell development (18).

Role of Other γ_c Cytokines in T Cell Development. To further explore the landscape of cytokine function in T cell development, we examined whether cytokines other than il7 (and the putative tslp equivalent) have roles in zebrafish T cell development. To this end, we first examined the expression patterns of *il2*, *il15*, *il15l*, and *il21* genes in the thymus by RNA in situ hybridization. Whereas expression of *il15l* could not be detected in the thymus, and only very few *il21*-positive cells were found, numerous cells expressed *il2* and *il15* (Fig. 5 *A* and *D*). As expected from their expression patterns in the thymus, *il15l* and *il21* morphants exhibited essentially normal T cell development (*SI Appendix*, Fig. S3 *A* and *B*); in contrast, both *il2* (Fig. 5 *B* and *C*) and *il15* (Fig. 5 *E* and *F*) morphants showed a strong reduction of the number of *rag1*-expressing thymocytes, as did *il15r* morphants (*SI Appendix*, Fig. S3*C*). Genetic interaction analyses were carried out between *il7r* (covering both il7 and the presumptive tslp cytokine receptor complexes), and the 2 thymopoietic cytokine genes *il2* and *il15*. Synthetic interactions were observed for both the *il2* and *il7r* (Fig. 5*G*) and *il15* and *il7r* (Fig. 5*H*) combinations. These findings suggest that *il7r* and the 2 cytokine genes encoding il2 and il15 function in parallel pathways to control T cell development and thus *il2* and *il15* appear to signal through receptor complexes not involving the il7r α chain.

Discussion

The moderate effect of *il7* deficiency on T cell development in zebrafish described here has led to the subsequent identification of the degenerate cytokine network underlying the development of T cells in the zebrafish thymus. Our studies show that in addition to *il7*, intrathymic T cell development in zebrafish requires *il2*, *il15*, and possibly other cytokine genes, such as that encoding a cytokine functionally equivalent to mammalian TSLP (Fig. 5*I*). This degeneracy stands in stark contrast to the brittle network configuration of its mammalian counterpart; here intrathymic T cell development depends almost entirely on the activity of IL-7. Of note, the phenotype of *Il2rg*/*Crlf2* double-deficient mice suggested a minor but recognizable contribution of Tslp to mammalian

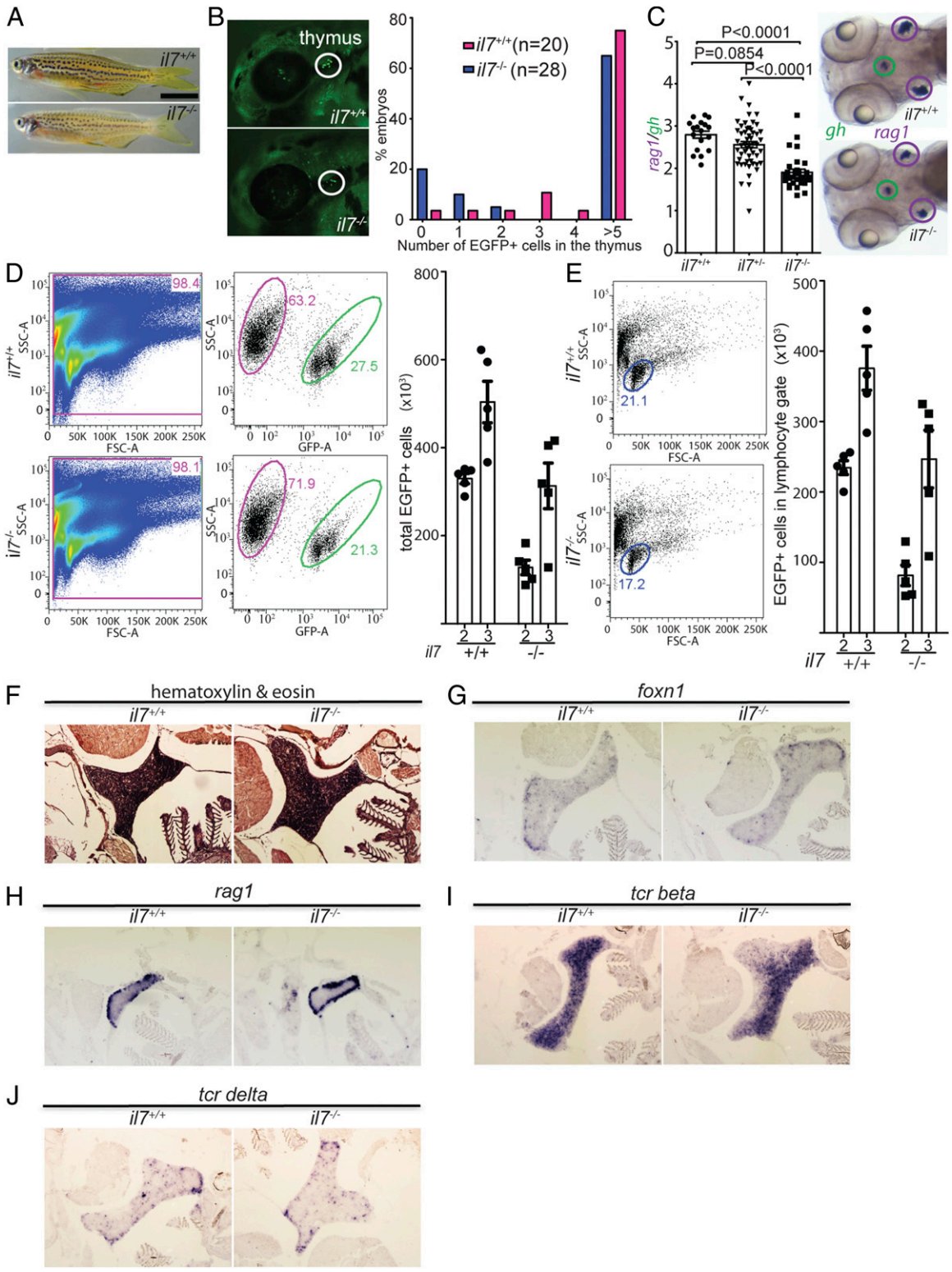

Fig. 2. Characterization of *il7* mutant zebrafish. (*A*) Normal gross appearance of adult wild-type (*il7*$^{+/+}$) and mutant (*il7*$^{-/-}$) fish. (*B*) Reduced number of *ikaros*-expressing lymphocytes in the thymus of *il7*-mutant fish also transgenic for an *ikaros:eGFP* reporter allele. (*Left*) Representative animals at 72 hpf. (*Right*) Quantitative assessment of cell numbers in the thymic rudiment. (*C*) Reduced thymopoietic activity in *il7* mutants as determined by the thymopoietic index (*Left*) derived from quantitative analysis of whole- mount RNA in situ hybridization experiments (*Right*). Each data point represents 1 fish; data are mean ± SEM. (*D*, *Left*) Flow cytometry analysis of GFP-positive cells present in the thymus of wild-type and *il7* mutant fish at age 2 mo. (*D*, *Right*) Enumeration of the total number of GFP-positive cells in the thymus at age 2 and 3 mo. Each data point represents 1 fish; data are mean ± SEM. (*E*) Enumeration of the total number of GFP-positive cells with light-scatter characteristics of lymphocytes (encircled; age 2 mo) (*Left*) in the thymus at age 2 and 3 mo (*Right*). Each data point represents 1 fish; data are mean ± SEM. A comparison of the data in *D* and *E* indicates that the majority of GFP-positive cells in the thymus are lymphocytes. (*F*) Normal histology of *il7* mutant thymus in adult fish. (*G*–*J*) RNA in situ hybridization on tissue sections of adult wild-type and *il7* mutant zebrafish thymus with probes specific for *foxn1* (*G*), expressed by thymic epithelial cells; *rag1* (*H*), indicative of immature thymocytes; *tcr beta* (*I*), indicative of αβ T cells; and *tcr delta* (*J*), indicative of γδ T cells.

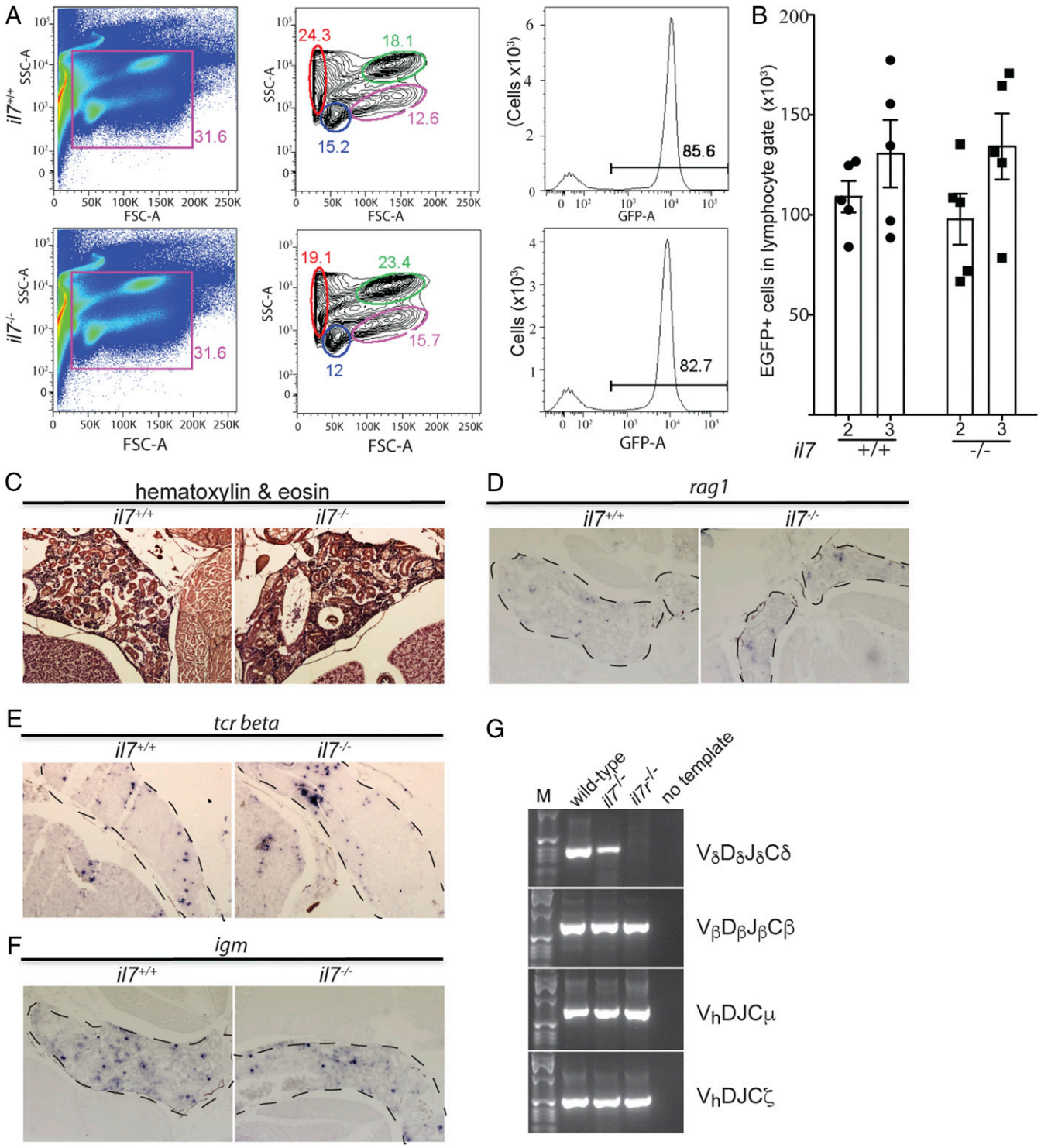

Fig. 3. Characterization of hematopoiesis in 3-mo-old zebrafish kidneys. (*A*) Flow cytometry analysis of cell populations in whole kidney marrow of adult wild-type and *il7*-mutant fish (*Left* and *Middle*). The different cell populations as identified by the characteristic light-scatter characteristics are indicated (red, erythrocytes; blue, lymphocytes; green, myeloid cells; pink, precursor cells) (34). The majority of cells in the lymphocyte gate (blue) are GFP-positive (*Right*). (*B*) Enumeration of GFP-positive cells in the lymphocyte gate of wild-type and *il7*-mutant fish at age 2 and 3 mo. Each data point represents 1 fish; data are mean ± SEM. (*C*) Normal histology of kidney marrow in *il7* mutant adult fish. (*D–F*) RNA in situ hybridization on tissue sections of adult wild-type and *il7* mutant kidney marrow (outlined with dashed lines) with probes specific for *rag1* (*D*), indicative of B cell precursors; *tcr beta* (*E*), indicative of αβ T cells; and *igm* (*F*), indicative of B cells. (*G*) RT-PCR assay for expressed completely assembled antigen receptor genes. Vd-Dd-Jd-Cd assemblies associated with the γδ T cell lineage are present in the whole kidney marrow of *il7* mutants but not in that of *il7r* mutants; assemblies of other lineage-specific antigen receptors are present in both mutant fish lines (Vb-Db-Jb-Cb for αβ T cells, Vh-D-J-Cm for Igμ-expressing B cells, and Vh-D-J-Cz for Igζ-expressing B cells). Representative panels are shown for wild-type fish ($n = 5$), *il7* mutants ($n = 4$), and *il7r* mutants ($n = 5$).

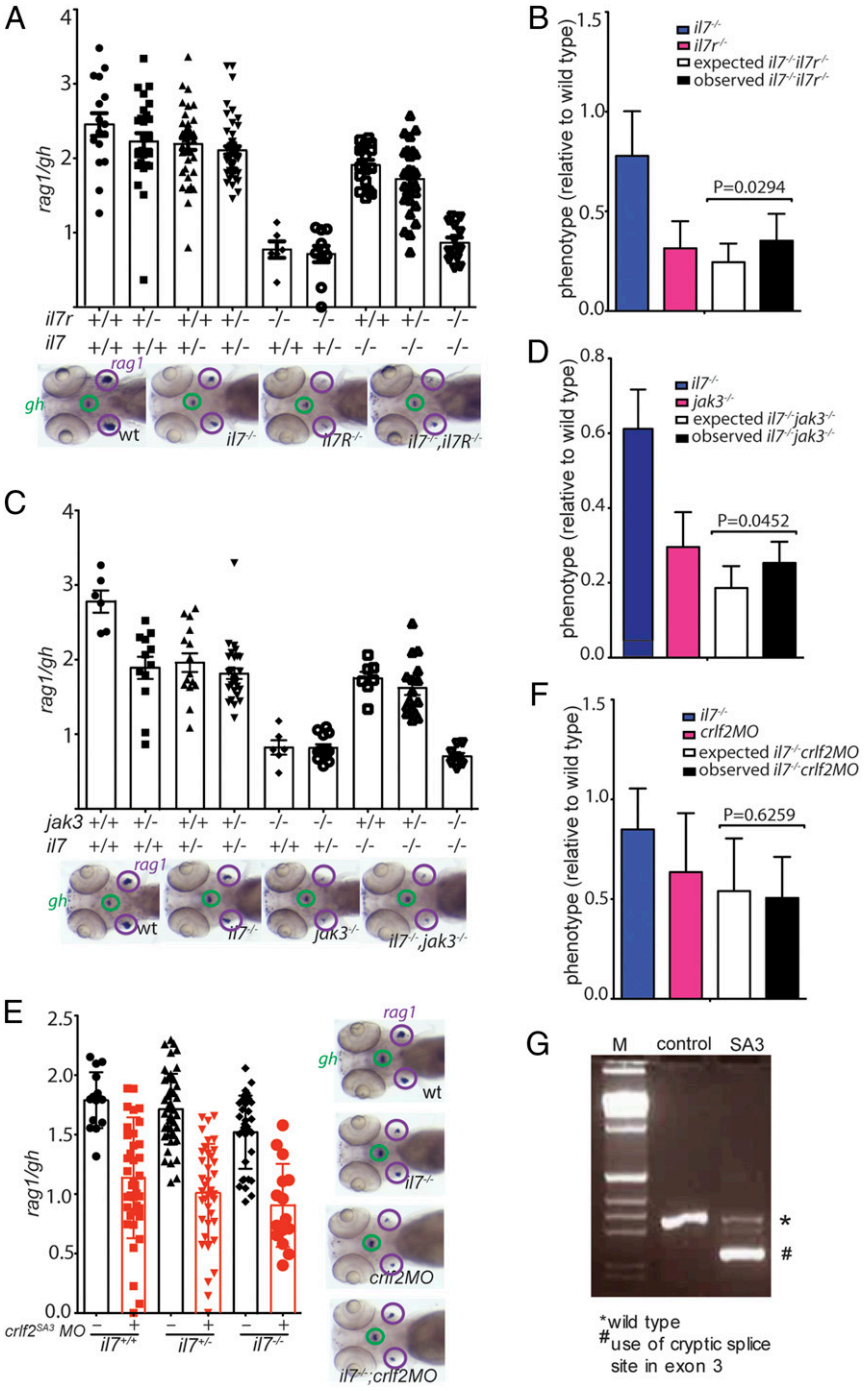

Fig. 4. Epistasis analysis of the *il7* mutation. (*A*) Thymopoietic capacities measured in fish of the 9 genotypes arising from an intercross of $il7^{+/-}$;$il7r^{+/-}$ double-heterozygous parents. Each data point represents 1 fish; data are mean ± SEM. Representative whole-mount RNA in situ hybridization results for the key genotypes are shown at the bottom. (*B*) Comparison of phenotypes of the 2 single mutants ($il7^{-/-}$ and $il7r^{-/-}$) and the $il7^{-/-}$;$il7r^{-/-}$ double mutant; the latter phenotype is compared with the expected phenotype (multiplicative model). The thymopoietic capacity observed in the double mutant is significantly higher than that expected from the combination of the single mutants, calculated under the assumption of no genetic interaction, indicative of alleviating genetic interaction. (*C*) Thymopoietic capacities measured in fish of the 9 genotypes arising from an intercross of $il7^{+/-}$;$jak3^{+/-}$ double-heterozygous parents. Each data point represents 1 fish; data are mean ± SEM. Representative whole-mount RNA in situ hybridization results for the key genotypes are shown at the bottom. (*D*) Comparison of phenotypes of the 2 single mutants ($il7^{-/-}$ and $jak3^{-/-}$) and the $il7^{-/-}$;$jak3^{-/-}$ double mutant with the expected phenotype. The observed thymopoietic capacity observed in the double mutant is significantly higher than that expected from the combination of the single mutants, indicative of alleviating genetic interaction. (*E*) Thymopoietic capacities measured in *crlf2* morphants of 3 different *il7* genotypes. Representative whole-mount RNA in situ hybridization results are shown at the right. (*F*) The degree of reduction of thymopoietic activity in the presence of the *crlf2* antisense oligonucleotide is independent of *il7* genotype, indicating that the 2 effects are genetically independent (no genetic interaction). (*G*) RT-PCR analysis of *crlf2* cDNA structures resulting from interference with splicing of the pre-mRNA transcripts by an antisense oligonucleotide targeting the splice donor site of exon 3 (SD3).

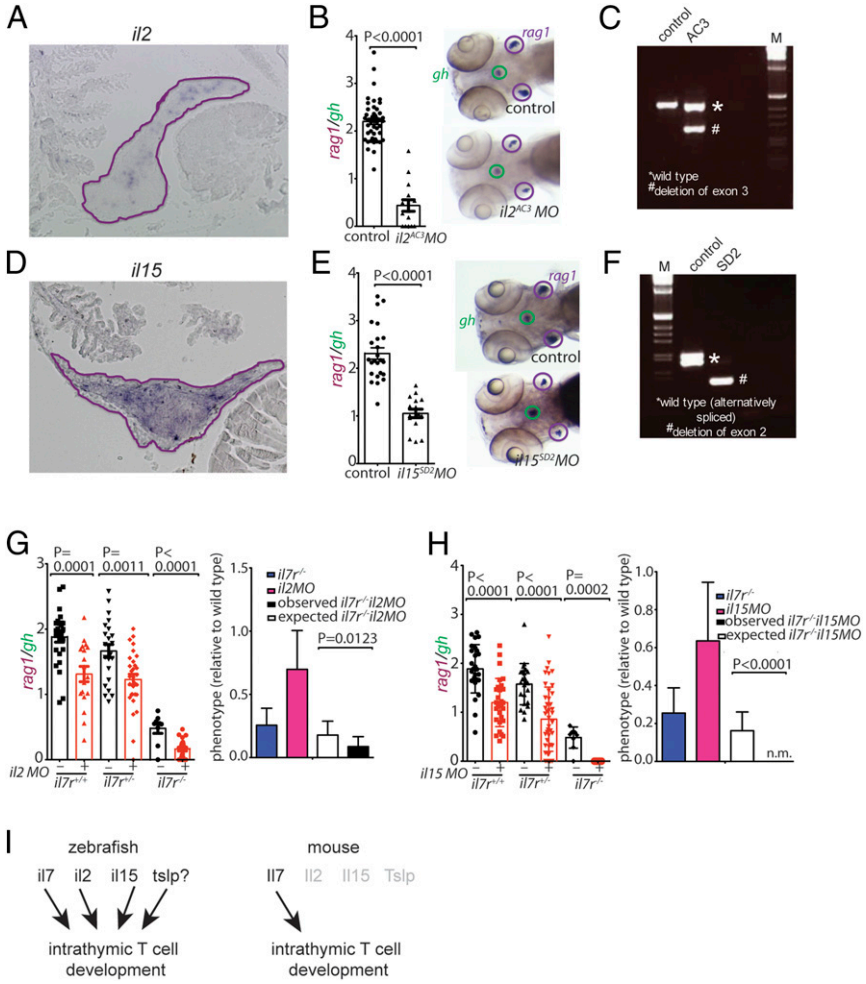

Fig. 5. Characterization of cytokine gene morphants. (*A*) RNA in situ hybridization on tissue sections of adult zebrafish thymus with probes specific for *il2*; the positive cells appear to cluster in certain regions of the thymus. (*B*) Reduced thymopoietic activity in *il2* morphants as determined by the thymopoietic index (*Left*), derived from quantitative analysis of whole-mount RNA in situ hybridization experiments (*Right*). Each data point represents 1 fish; data are mean ± SEM. (*C*) RT-PCR analysis of *il2* cDNA structures resulting from interference with splicing of the pre-mRNA transcripts by an antisense oligonucleotide targeting the splice acceptor site of exon 3 (AC3). (*D*) RNA in situ hybridization on tissue sections of adult zebrafish thymus with probes specific for *il15*. (*E*) Reduced thymopoietic activity in *il15* morphants as determined by the thymopoietic index (*Left*), derived from quantitative analysis of whole-mount RNA in situ hybridization experiments (*Right*). Each data point represents 1 fish; data are mean ± SEM. (*F*) RT-PCR analysis of *il15* cDNA structures resulting from interference with splicing of the pre-mRNA transcripts by an antisense oligonucleotide targeting the splice donor site of exon 2 (AC3). (*G*, *Left*) Thymopoietic capacities measured in *il2* morphants of 3 different *il7r* genotypes. Each data point represents 1 fish; data are mean ± SEM. (*G*, *Right*) The degree of thymopoietic activity in the presence of the *il2* antisense oligonucleotide is significantly lower than expected from neutrality, indicating the presence of synthetic genetic interaction between *il2* and *il7r*. (*H*, *Left*) Thymopoietic capacities measured in *il15* morphants of 3 different *il7r* genotypes. Each data point represents 1 fish; data are mean ± SEM. (*H*, *Right*) The degree of thymopoietic activity in the presence of the *il15* antisense oligonucleotide is significantly lower than that expected from neutrality (n.m. denotes the absence of detectable *rag1* signal in the double-mutant fish), indicating the presence of a synthetic genetic interaction between *il15* and *il7r*. (*I*) Schematic representation of the degenerate cytokine network regulating intrathymic T cell development in zebrafish (*Left*) and the corresponding nonredundant network structure in mouse (*Right*).

intrathymic T cell development (21), which we interpret as reflecting an evolutionary trace of the ancient degenerate network configuration.

From a systems perspective, our observations suggest that the degenerate zebrafish network has a higher degree of evolvability than that of mammals (22). Mammalian intrathymic T cell development relies on a nonredundant system of IL-7 signaling (with SCF also making only a minor contribution; ref. 1), since IL-7 deficiency drastically reduces the magnitude of T cell development in the thymus (2, 6). Thus, network functionality in mammals has arrived at an essentially all-or-none configuration. In such a situation, evolutionary adaptations are difficult to achieve, since in the absence of physiologically relevant backup activities, any changes in the ligand–receptor interactions carry the risk of generating catastrophic failure. Therefore, with respect to T cell development in the thymus, the system is essentially locked into the present state. In contrast, the degree of evolvability is much higher in a partially redundant (or degenerate) multicomponent system, in which many elements jointly contribute to the overall outcome of the network. While some components can maintain the original functions, other elements may be modified in response to new physiological circumstances. Such degeneracy appears to be present in the cytokine network regulating intrathymic T cell development in zebrafish, rendering the genetic network underlying the thymopoietic capacity of teleosts much more flexible.

Our present studies raise several questions about the functions of cytokines in the zebrafish immune system. We predict that zebrafish have at least 1 additional cytokine that signals through the il7r/crlf2 receptor pair and speculate that this cytokine is a

functional equivalent of the mammalian TSLP cytokine. However, so far we have been unable to identify related sequences in genomic and cDNA sequence collections; possible reasons are a high degree of sequence divergence (which is not uncommon for the rapidly evolving cytokines in general; see *SI Appendix*, Fig. S1 *D* and *E*) and/or low levels of expression. Compared with the situation in the mouse, it appears that the putative zebrafish tslp equivalent has a larger spectrum of activities, since *Tslp* deficiency in the mouse has little effect on the magnitude of intrathymic T cell development (21) but does affect regulatory functions in the peripheral immune system (20). Likewise, *Il2* deficiency in the mouse does not appreciably affect T cell development (23), but instead impairs peripheral immune homeostasis (24). Moreover, although *Il15* is important for CD8 T lineage specification in the thymus (25) and memory formation in the periphery (26), the effect of IL-15 and/or IL-15R deficiency on the total number of thymocytes is minimal (27, 28), in contrast to the situation in zebrafish described here. Once the putative zebrafish *tslp* equivalent is identified, its roles in T and B cell development and the peripheral immune system can be examined and compared with the phenotypes of fish deficient for *il2* and *il15* genes.

Our results suggest that a degenerate cytokine network of il7, il2, il15, and possibly of the tslp equivalent that collectively supports T cell development in teleosts has evolved into an essentially nonredundant configuration in mammals, in which IL-7 plays a dominant role (Fig. 5*I*). Whereas other cytokines can contribute to the regulation of T cell development, their impact varies among species; this becomes apparent when comparing the phenotypes of IL-7–deficient (6) and IL-7R–deficient (7) human patients and those of equivalent deficiencies in mice (2, 4).

At present, we can only speculate why the mammalian cytokine network regulating T cell development in the thymus has evolved to rely almost entirely on IL-7 as the lymphopoietic cytokine. It is possible that the higher demands on immune regulation in mammals required the repurposing of cytokines such as IL-2, IL-15, and IL-21 and their corresponding receptors for peripheral functions to achieve a more fine-tuned regulation of the immune response and/or maintenance of tolerance (29). If so, this would suggest that the basic building blocks of immune regulatory cytokines are used in different ways in lower vertebrates and in mammals. In this context, it will be interesting to address the structure of cytokine networks in the immune system of the sister group of jawed vertebrates, lampreys and hagfishes. These jawless vertebrates split off from the lineage giving rise to teleosts and mammals approximately 500 million years ago and exhibit an adaptive immune system based on alternative types of antigen receptors (30). Since the coding capacity of cytokines in this group of vertebrates has not yet been explored, it is difficult to predict whether T cell development in the thymus (31) operates under nonredundant (mammals) and degenerate (teleost) versions of the cytokine network.

Materials and Methods

Animals. The zebrafish (*Danio rerio*) wild-type strain TLEK (Tüpfel long fin/Ekkwill) is maintained in the animal facility of the Max Planck Institute of Immunobiology and Epigenetics in Freiburg, Germany. The *il7r* and *jak3* mutant lines have been described previously (10), as has the *ikaros:eGFP* transgenic reporter (17). All animal experiments were performed in accordance with relevant guidelines and regulations and approved by the Review Committee of the Max Planck Institute of Immunobiology and Epigenetics and the Regierungspräsidium Freiburg, Germany (license Az 35–9185.81/G-14/41).

Morphants. Morphants were generated by injection of antisense morpholino oligonucleotides (Gene Tools) to block the translation of both maternal and zygotic mRNAs ("ATG morpholinos") or block splicing of zygotic pre-mRNAs ("splice morpholinos"). Stock solutions were diluted as required; the final concentration in the injection buffer (0.05% vol/vol phenol red and 1× Danieau buffer; http://cshprotocols.cshlp.org/content/2011/7/pdb.rec12467.full) is shown in *SI Appendix*, Table S2. Approximately 1 to 2 nL of solution was injected into fertilized eggs as described previously (32). The morphants (*SI Appendix*, Table S2) were analyzed at 5 dpf by RNA in situ hybridization using a combination of *rag1*- and *gh*-specific probes, with the results expressed as a thymopoietic index, a dimensionless figure (see below), and by RT-PCR to determine the structure of aberrant splice products, followed by sequence determination of the resulting amplicons (*SI Appendix*, Table S2).

Thymopoietic Index. Thymic *rag1* gene expression is a marker of ongoing assembly of T cell receptor genes. Thus, the intensity of the RNA in situ signal correlates with the number of differentiating T cells, which we consider to be a measure of T cell development. To provide an internal control (technical, with respect to the hybridization process as such, and biological, with respect to the tissue specificity of the observed genetic effects), we used a probe specific for the growth hormone (*gh*) gene, which marks a subset of cells in the hypophysis. Determination of *rag1*/*gh* ratios was carried out as follows. After RNA in situ hybridization with *rag1* and *gh* probes, ventral images of 4 to 5 dpf zebrafish larvae were obtained with a Leica MZFLIII microscope and a Leica DFC300FX digital camera, essentially generating a 2D projection of the 3D structure. The areas of *rag1* and *gh* signals were measured using ImageJ, and the ratio of average of the *rag1*-positive area vs. *gh*-positive area was calculated as a measure of thymopoietic activity. After photographic documentation of the RNA in situ hybridization signal, larvae were processed for genomic DNA extraction for subsequent genotyping.

RNA Extraction and cDNA Synthesis. Total RNA was extracted using TRI Reagent (Sigma-Aldrich) following the manufacturer's instructions. After treatment with DNaseI (Promega), RNA extraction using TRI Reagent was repeated. Superscript II Reverse Transcriptase (Invitrogen) and oligo(dT) were used for cDNA synthesis from total RNA.

RNA in Situ Probes. (a) The probe for *il7* was generated by nested RT-PCR using the following primers: first round, il7rt_F1: 5′-TTCCTCAGTCAAATCCTGAATC, il7rt_R1: 5′-CAGTTACGCACTTGACGTTCT; second round, il7rt_F2a: 5′-CTCCGACGATACAATGCGAC, il7rt_R2: 5′-CCTGAATCTTGTGAATGTTGCA. (b) The probe for *il2* was generated using the following primers: first round, il2_F1: 5′-CGCACACACTGATGATGATGA, il2_R1: 5′-TTCTGCCTCCATTCGTTCATC; second round, il2_F2: 5′-AGGATGTCTGCTCTACACTG, il2_R2: 5′-ACGTTCTTCAGGAACGTCATG. (c) The probe for *il21* was generated using the following primers: first round, il21_F1: 5′-ACGCGCCTCTCGATTACATC, il21_R1: 5′- GAGATTTCACCACACGGTGG; second round, il21_F2: 5′-AGGTGATCGAGCACCTGTGT, il21_R2: 5′-GCTTAGCAGCCCAGTTTCTC. (d) The probe for *il15l* was generated using the following primers: first round, il15l_F1: 5′-AACAATGAGCGGGTGACGAC, il15l_R1: 5′-CCTCTGGAGAAGCACTTCAG; second round, il15l_F2: 5′-GACGACTCGGCTTTCGATAG, il15l_R2: 5′-CAGAACCGCTCCTTCAGATC. (e) The zebrafish *il15* cDNA is equivalent to IMAGE clone 7990051 (GenBank accession no. BC133847.1). (f) The *rag1*, *gh, tcrb, tcrd,* and *igm* probes were as described previously (32).

***il7* Mutagenesis.** A deletion in the *il7* locus was generated by injection of 2 RNPs containing Cas9 protein and sgRNAs. The injection solution contained (final concentrations) 12.5 to 50 ng/μL sgRNAs, 500 ng/μL Cas9 protein (PNA Bio), and 0.05% (vol/vol) phenol red, in 1× Danieau buffer (http://cshprotocols.cshlp.org/content/2011/7/pdb.rec12467.full). Approximately 1 to 2 nL of the solution was injected into fertilized embryos. The target sequences of the 2 sgRNAs were as follows: sgRNA_1: 5′-AATGACAAATGGTAAGCTGA (position in genome, nt 22,731,430 on chromosome 24) and sgRNA_2: 5′-AAAGGTAACTGAAACAACCC (position in genome, nt 22,733,214 on chromosome 24); coordinates refer to GRCZ11. The sequences around the breakpoint are shown in *SI Appendix*, Fig. S1; note that a total 16 nontemplated nucleotides were inserted into the genome between the 2 break points.

Analysis of *il7* cDNA Isoforms. Nested RT-PCR was used to examine the structure of the various isoforms of *il7* transcripts. For isoforms 1, 2, and 3 (*SI Appendix*, Fig. S1*B*), the following primers were used: first round, il7rt_F1: 5′-CAGTTACGCACTTGACGTTCT, il7rt_R2: 5′-CCTGAATCTTGTGAATGTTGCA; second round, il7_F2: 5′-CGAAGCGATATAGCCCCATC, il7rt_R3 5′-TTGTGAATGTTGCAAAGTGGGT. For isoform 4, the following primers were used: first round, il7exon1a_F1: 5′-GCGTACGCTTACCTTGACGA, il7rt_R2: 5′-CCTGAATCTTGTGAATGTTGCA; second round, il7exon1a_F2: 5′-TTTGGAGGAGGACGACAGGA, il7rt_R3: 5′-TTGTGAATGTTGCAAAGTGGGT.

Ag Receptor Gene Assembly. Nested RT-PCR assays were used to examine the presence of transcribed assembled antigen receptor genes as described previously (32).

RNA-Seq Analyses. For differential gene expression analysis, RNA was extracted from whole kidney marrow (wild-type and *il7*-deficient animals; $n = 3$ each). The libraries were sequenced in paired-end 75-bp mode on an Illumina HiSeq 2500 instrument. The high-throughput RNA sequencing analysis pipeline and the relevant statistical models used are essentially as described previously (9). RNA-seq data have been deposited in the Gene Expression Omnibus database (33).

Statistical Analysis. Two-tailed *t* tests were used to determine the significance levels of the differences between the means of 2 independent samples, considering equal or unequal variances as determined by the *F* test. For multiple tests, Bonferroni correction was applied.

ACKNOWLEDGMENTS. We thank Christine Strohmeier for help with RNA in situ hybridization experiments and the staff of the Deep Sequencing Unit of the Max Planck Institute of Immunobiology and Epigenetics for next-generation sequencing. This work was supported by the Max Planck Society and the European Research Council (ERC) under the European Union's Seventh Framework Programme (FP7/2007-2013), ERC Grant Agreement 323126.

1. J. P. Di Santo, H.-R. Rodewald, In vivo roles of receptor tyrosine kinases and cytokine receptors in early thymocyte development. *Curr. Opin. Immunol.* **10**, 196–207 (1998).
2. U. von Freeden-Jeffry *et al*., Lymphopenia in interleukin (IL)-7 gene-deleted mice identifies IL-7 as a nonredundant cytokine. *J. Exp. Med.* **181**, 1519–1526 (1995).
3. J. X. Lin, W. J. Leonard, The common cytokine receptor γ chain family of cytokines. *Cold Spring Harb. Perspect. Biol.* **10**, a028449 (2018).
4. J. J. Peschon *et al*., Early lymphocyte expansion is severely impaired in interleukin 7 receptor-deficient mice. *J. Exp. Med.* **180**, 1955–1960 (1994).
5. J. P. DiSanto, W. Müller, D. Guy-Grand, A. Fischer, K. Rajewsky, Lymphoid development in mice with a targeted deletion of the interleukin 2 receptor gamma chain. *Proc. Natl. Acad. Sci. U.S.A.* **92**, 377–381 (1995).
6. L. Horev *et al*., Generalized verrucosis and HPV-3 susceptibility associated with CD4 T-cell lymphopenia caused by inherited human interleukin-7 deficiency. *J. Am. Acad. Dermatol.* **72**, 1082–1084 (2015).
7. A. Puel, S. F. Ziegler, R. H. Buckley, W. J. Leonard, Defective IL7R expression in T(-)B(+)NK(+) severe combined immunodeficiency. *Nat. Genet.* **20**, 394–397 (1998).
8. M. Noguchi *et al*., Interleukin-2 receptor gamma chain mutation results in X-linked severe combined immunodeficiency in humans. *Cell* **73**, 147–157 (1993).
9. N. Iwanami *et al*., Forward genetic screens in zebrafish identify pre-mRNA-processing pathways regulating early T cell development. *Cell Rep.* **17**, 2259–2270 (2016).
10. N. Iwanami *et al*., Genetic evidence for an evolutionarily conserved role of IL-7 signaling in T cell development of zebrafish. *J. Immunol.* **186**, 7060–7066 (2011).
11. R. Sertori *et al*., Conserved IL-2Rγc signaling mediates lymphopoiesis in zebrafish. *J. Immunol.* **196**, 135–143 (2016).
12. M. Nehls, D. Pfeifer, M. Schorpp, H. Hedrich, T. Boehm, New member of the winged-helix protein family disrupted in mouse and rat nude mutations. *Nature* **372**, 103–107 (1994).
13. M. Nehls *et al*., Two genetically separable steps in the differentiation of thymic epithelium. *Science* **272**, 886–889 (1996).
14. L. Calderón, T. Boehm, Synergistic, context-dependent, and hierarchical functions of epithelial components in thymic microenvironments. *Cell* **149**, 159–172 (2012).
15. J. B. Swann *et al*., Conversion of the thymus into a bipotent lymphoid organ by replacement of *FOXN1* with its paralog, *FOXN4*. *Cell Rep.* **8**, 1184–1197 (2014).
16. B. Venkatesh *et al*., Elephant shark genome provides unique insights into gnathostome evolution. *Nature* **505**, 174–179 (2014).
17. I. Hess, T. Boehm, Intravital imaging of thymopoiesis reveals dynamic lympho-epithelial interactions. *Immunity* **36**, 298–309 (2012).
18. T. A. Moore, U. von Freeden-Jeffry, R. Murray, A. Zlotnik, Inhibition of gamma delta T cell development and early thymocyte maturation in IL-7$^{-/-}$ mice. *J. Immunol.* **157**, 2366–2373 (1996).
19. A. Baryshnikova, M. Costanzo, C. L. Myers, B. Andrews, C. Boone, Genetic interaction networks: Toward an understanding of heritability. *Annu. Rev. Genomics Hum. Genet.* **14**, 111–133 (2013).
20. S. F. Ziegler, Y.-J. Liu, Thymic stromal lymphopoietin in normal and pathogenic T cell development and function. *Nat. Immunol.* **7**, 709–714 (2006).
21. A. Al-Shami *et al*., A role for thymic stromal lymphopoietin in CD4(+) T cell development. *J. Exp. Med.* **200**, 159–168 (2004).
22. G. Tononi, O. Sporns, G. M. Edelman, Measures of degeneracy and redundancy in biological networks. *Proc. Natl. Acad. Sci. U.S.A.* **96**, 3257–3262 (1999).
23. H. Schorle, T. Holtschke, T. Hünig, A. Schimpl, I. Horak, Development and function of T cells in mice rendered interleukin-2 deficient by gene targeting. *Nature* **352**, 621–624 (1991).
24. B. Sadlack *et al*., Ulcerative colitis-like disease in mice with a disrupted interleukin-2 gene. *Cell* **75**, 253–261 (1993).
25. R. Etzensperger *et al*., Identification of lineage-specifying cytokines that signal all CD8^{+}-cytotoxic-lineage-fate "decisions" in the thymus. *Nat. Immunol.* **18**, 1218–1227 (2017).
26. C. D. Surh, J. Sprent, Regulation of mature T cell homeostasis. *Semin. Immunol.* **17**, 183–191 (2005).
27. M. K. Kennedy *et al*., Reversible defects in natural killer and memory CD8 T cell lineages in interleukin 15-deficient mice. *J. Exp. Med.* **191**, 771–780 (2000).
28. J. P. Lodolce *et al*., IL-15 receptor maintains lymphoid homeostasis by supporting lymphocyte homing and proliferation. *Immunity* **9**, 669–676 (1998).
29. W. J. Leonard, J. X. Lin, J. J. O'Shea, The γ_c family of cytokines: Basic biology to therapeutic ramifications. *Immunity* **50**, 832–850 (2019).
30. Z. Pancer *et al*., Somatic diversification of variable lymphocyte receptors in the agnathan sea lamprey. *Nature* **430**, 174–180 (2004).
31. B. Bajoghli *et al*., A thymus candidate in lampreys. *Nature* **470**, 90–94 (2011).
32. M. Schorpp *et al*., Conserved functions of Ikaros in vertebrate lymphocyte development: Genetic evidence for distinct larval and adult phases of T cell development and two lineages of B cells in zebrafish. *J. Immunol.* **177**, 2463–2476 (2006).
33. R. Edgar, M. Domrachev, A. E. Lash, Gene Expression Omnibus: NCBI gene expression and hybridization array data repository. *Nucleic Acids Res.* **30**, 207–210 (2002).
34. D. Traver *et al*., Transplantation and *in vivo* imaging of multilineage engraftment in zebrafish bloodless mutants. *Nat. Immunol.* **4**, 1238–1246 (2003).